Co2FeAl Heusler thin films grown on Si and MgO substrates: Annealing temperature effect

M. Belmeguenai, H. Tuzcuoglu, M. S. Gabor, T. Petrisor Jr., C. Tiusan, F. Zighem, S. M. Chérif, and P. Moch

Citation: Journal of Applied Physics **115**, 043918 (2014); doi: 10.1063/1.4863398
View online: http://dx.doi.org/10.1063/1.4863398
View Table of Contents: http://scitation.aip.org/content/aip/journal/jap/115/4?ver=pdfcov
Published by the AIP Publishing

Co_2FeAl Heusler thin films grown on Si and MgO substrates: Annealing temperature effect

M. Belmeguenai,[1,a)] H. Tuzcuoglu,[1] M. S. Gabor,[2,b)] T. Petrisor, Jr.,[2] C. Tiusan,[2,3] F. Zighem,[1] S. M. Chérif,[1] and P. Moch[1]
[1]*LSPM (CNRS-UPR 3407), 99 avenue Jean-Baptiste Clément, Université Paris 13, 93430 Villetaneuse, France*
[2]*Center for Superconductivity, Spintronics and Surface Science, Technical University of Cluj-Napoca, Str. Memorandumului No. 28 RO-400114 Cluj-Napoca, Romania*
[3]*Institut Jean Lamour, CNRS, Université de Nancy, BP 70239, F–54506 Vandoeuvre, France*

(Received 30 October 2013; accepted 14 January 2014; published online 29 January 2014)

10 nm and 50 nm Co_2FeAl (CFA) thin films have been deposited on MgO(001) and Si(001) substrates by magnetron sputtering and annealed at different temperatures. X-rays diffraction revealed polycrystalline or epitaxial growth (according to CFA(001)[110]//MgO(001)[100] epitaxial relation) for CFA films grown on a Si and on a MgO substrate, respectively. For these later, the chemical order varies from the A2 phase to the B2 phase when increasing the annealing temperature (T_a), while only the A2 disorder type has been observed for CFA grown on Si. Microstrip ferromagnetic resonance (MS-FMR) measurements revealed that the in-plane anisotropy results from the superposition of a uniaxial and a fourfold symmetry term for CFA grown on MgO substrates. This fourfold anisotropy, which disappears completely for samples grown on Si, is in accord with the crystal structure of the samples. The fourfold anisotropy field decreases when increasing T_a, while the uniaxial anisotropy field is nearly unaffected by T_a within the investigated range. The MS-FMR data also allow for concluding that the gyromagnetic factor remains constant and that the exchange stiffness constant increases with T_a. Finally, the FMR linewidth decreases when increasing T_a, due to the enhancement of the chemical order. We derive a very low intrinsic damping parameter (1.1×10^{-3} and 1.3×10^{-3} for films of 50 nm thickness annealed at 615 °C grown on MgO and on Si, respectively). © *2014 AIP Publishing LLC*. [http://dx.doi.org/10.1063/1.4863398]

I. INTRODUCTION

The future spintronic devices require ideal spin-polarized electron sources, achievable by using a half-metallic Heusler alloy,[1,2] having the composition X_2YZ (X being a transition metal element, Y being another transition metal element, and Z being a group III, IV, or V element). These materials are expected to provide very large magneto-resistive effects when used as magnetic electrodes in magnetic tunnel junctions (MTJs) and in current-perpendicular-to-plane (CPP) spin valves. They can be used as perfect spin filters and spin-injection devices as alternative materials to ferromagnetic 3*d* metals. Therefore, Co-based Heusler alloys, such as Co_2FeAl (CFA), have attracted much research interest due to their large magnetic moment and their high Curie temperature. CFA has a very high Curie temperature (1000 K) and is theoretically predicted to have a half-metallic character arising from its spin-split band structure. It can provide giant tunnelling magneto-resistance (360% at room temperature (RT))[3,4] when used as an electrode in magnetic tunnel junctions, which makes CFA promising for practical applications. However in such alloys, there is always some degree of chemical disorder, which strongly influences many of their physical properties. In reality, the totally ordered phase ($L2_1$) is difficult to achieve and there is a variety of derived structural types arising from atomic disorder in the occupation of the available sites. When the X atoms occupy their assigned sites for the $L2_1$ phase, while the Y and Z atoms randomly share the other ones, the B2 structure is obtained. The structure A2 corresponds to a completely random occupation, by any X, Y, or Z atom, of all the existing sites of the $L2_1$ phase. It is reported by Picozzi that some types of disorder might lead to additional states at the Fermi level, thus reducing the spin polarization.[5] In addition to the atomic order, the crystallographic orientation of the Heusler thin film is important and may break the half metallicity. Therefore, an annealing process is required to initiate the crystallization and to induce the atomic ordering. It is thus of great interest to investigate the annealing temperature (T_a) effects on the structural and magnetic properties of CFA thin films.

The purpose of this paper is to use ferromagnetic resonance in microstrip line (MS-FMR) under an in-plane and an out-of-plane applied magnetic field, combined to vibrating sample magnetometry (VSM), in view of investigating the correlation between structural and magnetic properties of CFA thin films grown on Si or on MgO substrates and annealed at different temperatures. A special attention will be given to the effect of T_a on the FMR linewidth and damping constant.

II. SAMPLE AND EXPERIMENTAL SET UP

CFA films were grown on MgO(001) and thermally oxidized Si(001)/SiO_2 substrates using a magnetron sputtering system with a base pressure lower than 3×10^{-9} Torr. Prior

a)belmeguenai.mohamed@univ-paris13.fr
b)mihai.gabor@phys.utcluj.ro

to the deposition of the CFA films, a 4 nm thick MgO buffer layer was grown at RT by RF sputtering from a MgO polycrystalline target under an Argon pressure of 15 mTorr. Next, 10 nm and 50 nm thick CFA films were deposited at room temperature by DC sputtering under an Argon pressure of 1 mTorr, at a rate of 0.1 nm/s. Finally, the CFA films were capped with a MgO(4 nm)/Ta(4 nm) bilayer. After the growth of the stack, the structures were *ex-situ* annealed at different temperatures ($T_a = 315\,^\circ C$, $415\,^\circ C$, $515\,^\circ C$, and $615\,^\circ C$) for 15 min in vacuum.

The structural properties of the samples have been characterized by X-ray diffraction (XRD) using a four-circle diffractometer. Their magnetic static and dynamic properties have been studied by VSM and MS-FMR,[6] respectively.

III. STRUCTURAL PROPERTIES

XRD is a standard method for the characterization of the crystal growth properties of thin films. Figure 1 shows the XRD θ-2θ patterns for 50 nm thick CFA films grown on MgO substrates, annealed at different temperatures, and on Si substrates (grazing incidence (GI) configuration) annealed at $615\,^\circ C$. The XRD patterns show that in addition to the (002) peak of the MgO substrate, the CFA films (Fig. 1(a)) exhibit only two peaks which are attributed to the (002) and (004) diffraction lines of CFA. The (004) peak is expected for the A2 type structure, while the existence of an additional (002) peak indicates a B2 type structure. Since the ratio I_{002}/I_{004} of the integrated intensities of the (002) and of the (004) peaks increases versus T_a (Fig. 1(c)), the chemical order varies from the B2 phase towards the A2 phase when decreasing T_a.[7] However, the I_{002}/I_{004} ratio is significantly below the theoretical expected one for a fully B2 ordered crystal.[8] This suggests that in the studied sample annealed at $615\,^\circ C$, at least part of the film keeps a significant chemical disorder and that some amorphous regions are presumably present. Moreover, from the analysis of the X-ray data using the Scherrer equation, we deduced that the films grown on MgO mainly consist of an assembly of crystallites showing a mean size of about 10 nm whatever the annealing temperature is. The X-ray measurements argue for a non-negligible dispersion of the chemical order among the crystallites. This dispersion as well as the relative amount of amorphous regions evolves versus temperature. A transmission electron microscopy study would presumably allow for an improved microstructural characterization. Qualitatively, the increase of I_{004} and of I_{002}/I_{004} versus T_a respectively indicates an increase in the crystallized area and an increase in the chemical order but these processes are not completely achieved at $615\,^\circ C$.

In contrast, the GIXRD pattern of CFA films grown on Si (Fig. 1(b)) clearly shows peaks corresponding to CFA (022), (004), and (224) reflections, due to the lack of epitaxial growth in the case of a Si substrate, which gives rise to a polycrystalline structure. The diffraction patterns exhibit peaks (hkl) corresponding only to the $h + k + l = 4n$ (where n is an integer) type reflections which seems to indicate that the films show A2 structure with a disorder among Co, Fe, and Al sites. However, a precise evaluation of the chemical order is difficult to perform, due to the relative rather low diffracted signal. Furthermore, pole figures (not shown here) revealed that CFA grown on Si does not display any in-plane preferential growth direction. In the case of films grown on MgO,

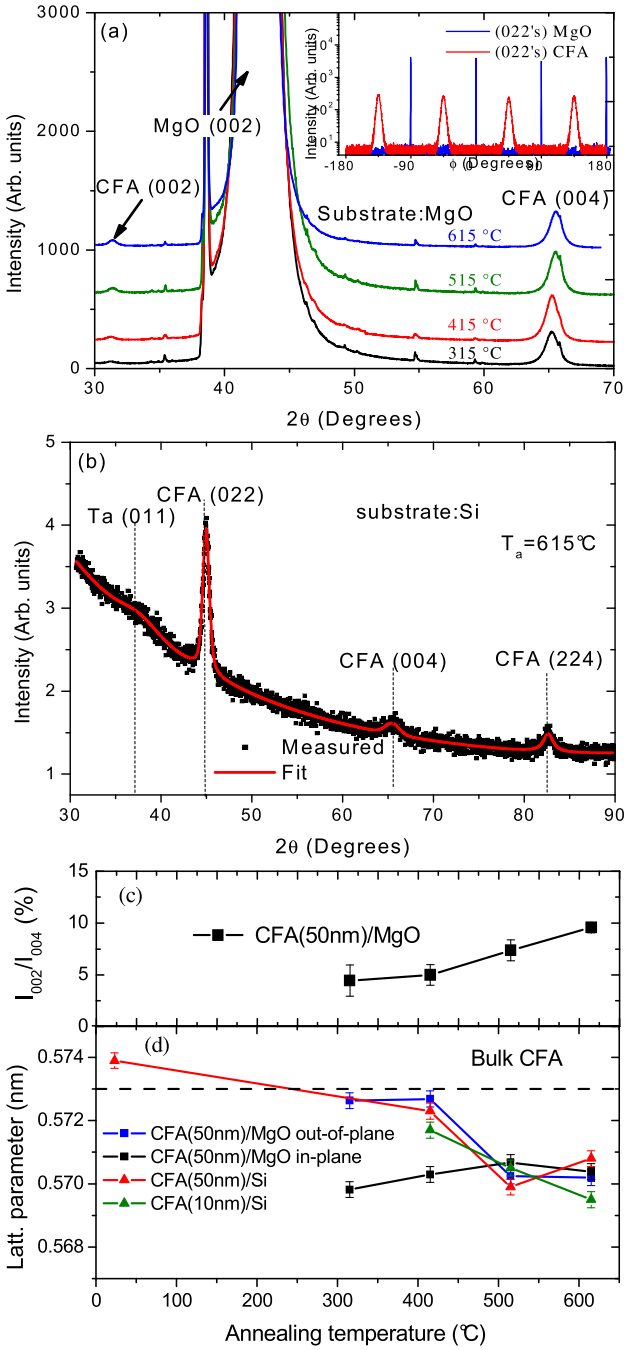

FIG. 1. (a) X−ray θ-2θ diffraction pattern for the 50 nm CFA thick films grown on a MgO substrate annealed at different temperatures. The inset represents the ϕ-scans of the substrate and the CFA films annealed at $615\,^\circ C$. (b) X-ray diffraction pattern measured in grazing incidence geometry for the 50 nm CFA thick film grown on a Si substrate annealed at $615\,^\circ C$. The symbols represent experimental data, while the lines are the result of the theoretical fit. The vertical dashed lines mark the positions of the Ta(011) and CFA((022), (004), (224)) reflections. (c) Evolution of the ratio, I_{002}/I_{004}, of the integral intensities of the (002) and (004) Co_2FeAl peaks versus the annealing temperature of 50 nm thick Co_2FeAl films grown on MgO Substrates. (d) Evolution of the lattice parameter as function of the annealing temperature in 10 nm and 50 nm thick Co_2FeAl films grown on Si and MgO substrates.

ϕ-scan measurements (see inset of Fig. 1(a)) allow for asserting their epitaxial growth within the investigated annealing temperature range, according to the expected CFA(001)[110]//MgO(001)[100] epitaxial relation.

Figure 1(d) shows the variations of the lattice constant for increasing annealing temperatures for different samples. The dashed line represents its value for bulk $L2_1$ ordered CFA.[9] For the films deposited on thermally oxidized $Si(001)/SiO_2$ substrates, the lattice constant was obtained from the observed (022) peak by applying the Bragg equation. In the as prepared state, the lattice parameter is larger than the reference bulk value and, for both substrates; it decreases with the increasing annealing temperatures. For films grown on MgO, both out-of-plane and in-plane lattice parameters were evaluated, using symmetric and asymmetric XRD scans relative to (004) and (022) reflections, respectively. From Fig. 1(d), one can observe that the as-deposited film experiences a relatively strong tetragonal distortion. As the annealing temperature increases, this distortion relaxes: for the films annealed at temperatures higher than 515 °C, the out-of-plane and the in-plane lattice parameters show practically identical values. Such an evolution in CFA/MgO(001) samples was previously noticed[7] and the tetragonal distortion was attributed to residual strains resulting from the growth method. Unfortunately, in the case of films deposited on thermally oxidized $Si(001)/SiO_2$ substrates, their polycrystalline character does not allow for such a detailed study and only a mean out-of-plane parameter is available. However, we have observed that the lattice parameters of films of identical thicknesses (50 nm) grown on Si or on MgO substrates are very close to each other in the investigated T_a range, suggesting that, in both cases, the decrease in the lattice parameter is mainly due to residual strains.

IV. MAGNETIC PROPERTIES

All the measurements presented here have been made at room temperature and analyzed using a model based on the following energy density, which was previously found to be appropriate to describe the properties of Heusler films[10]

$$\begin{aligned} E = & -M_s H[\cos(\varphi_M - \varphi_H)\sin\theta_M \sin\theta_H + \cos\theta_M \cos\theta_H] \\ & -\frac{1}{2}[1+\cos 2(\varphi_M - \varphi_u)]K_u \sin^2\theta_M \\ & -(2\pi M_s^2 - K_\perp)\sin^2\theta_M \\ & -\frac{1}{8}[3+\cos 4(\varphi_M - \varphi_4)]K_4 \sin^4\theta_M. \end{aligned} \quad (1)$$

In the above expression, θ_M and φ_M, respectively, represent the out-of-plane and the in-plane (referring to the substrate edges) angles defining the direction of the magnetization $\boldsymbol{M_s}$. φ_u and φ_4 define the angles between an easy uniaxial planar axis or an easy planar fourfold axis, respectively, with respect to this substrate edge. K_u, K_4, and $K_\perp$ are in-plane uniaxial, fourfold, and out-of-plane uniaxial anisotropy constants, respectively. We define $H_u = \frac{2K_u}{M_s}$ and $H_4 = \frac{4K_4}{M_s}$ as the in-plane uniaxial and the fourfold anisotropy fields, respectively, and we introduce the effective magnetization $M_{eff} = H_{eff}/4\pi$ obtained by

$$4\pi M_{eff} = H_{eff} = 4\pi M_s - \frac{2K_\perp}{M_s} = 4\pi M_s - H_\perp.$$

The resonance frequency expressions of the uniform precession mode and of the perpendicular standing spin waves (PSSW) modes assuming in-plane or perpendicular applied magnetic fields are given in Ref. 6. The experimental results concerning the measured peak-to-peak FMR linewidths (ΔH^{PP}) are analyzed in this work taking account of both intrinsic and extrinsic mechanisms. As discussed in Ref. 6, the observed magnetic field linewidth (ΔH^{PP}) is analyzed by considering Gilbert (ΔH^{Gi}),[11] inhomogeneities (ΔH^{inh}), and two magnon scattering (ΔH^{2mag})[12] contributions. This latter is given by[6]

$$\begin{aligned} \Delta H^{2mag} = & (\Gamma_0 + \Gamma_2 \cos 2(\varphi_H - \varphi_2) \\ & + \Gamma_4 \cos 4(\varphi_H - \varphi_4))\arcsin\left(\frac{f}{\sqrt{f^2 + f_0^2} + f_0}\right) \end{aligned} \quad (2)$$

with $f_0 = \gamma M_{eff}$. The expected fourfold symmetry induces the Γ_4 coefficient and contributes to Γ_0; the coefficient Γ_2 is phenomenologically introduced.

The total FMR linewidth in our samples can be written as follows:

$$\Delta H^{PP} = \Delta H^{Gi} + (\Delta H^{inh} + \Delta H^{2mag}). \quad (3)$$

The analysis of the variation of the FMR linewidth ΔH^{PP} versus the frequency and the in-plane field orientation allows for evaluating the Gilbert coefficient (α), ΔH^{inh}, Γ_0, Γ_2 (and φ_2), and Γ_4 (and φ_4 which, from symmetry considerations, is expected to have a 0° or 45° value, depending upon the chosen sign of Γ_4).

A. Static properties

The easy axis VSM hysteresis loops were measured at different field orientations, and the magnetization at saturation has been extracted. The magnetization at saturation of the three samples (not shown here) increases slightly (10% of change) with increasing T_a, which indicates an improved atomic ordering. A maximum value of 1029 emu/cm^3 can be achieved for a 50 nm CFA thick film grown on a MgO substrate and annealed at 615 °C. This value is higher, when compared with a similar CFA film grown on a Si substrate, most probably due to the higher crystalline quality and higher order degree.

Figure 2 shows typical hysteresis loops, along the easy axis, as function of the annealing temperature for the 50 nm thick CFA films grown on Si and on MgO substrates. For both substrates, a clearly different behaviour is observed between the samples annealed at low and at higher temperature. The increase in the coercive field (H_c) with decreasing T_a is an indication of the improved crystalline structure and of the chemical order in the annealed samples. One should

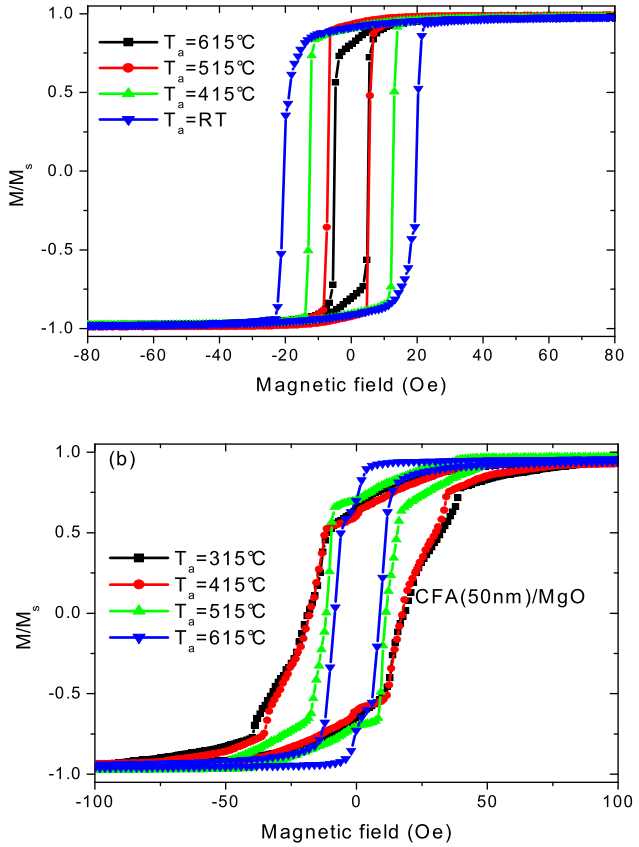

FIG. 2. Hysteresis loops, along the easy axis, of the 50 nm thick CFA films annealed at different temperatures and grown on (a) a Si substrate and on (b) a MgO Substrate.

mention that the angular dependence of M_r/M_s (not shown here) of annealed CFA films grown on Si showed a uniaxial anisotropy behaviour. As the annealing temperature increases, the sample quality and the chemical order are enhanced and a unique uniaxial anisotropy is observed. This is confirmed by the variation of the uniaxial anisotropy easy axis direction with T_a as shown below. For the 50 nm thick films grown on a MgO substrate, the measured hysteresis loops revealed a fourfold in-plane magnetic anisotropy with (110) easy and (100) hard axis directions to which a weak uniaxial magnetic anisotropy is superimposed. The intermixing of regions showing different chemical orders or, even, of amorphous regions, as revealed by XRD, generates areas showing different magnetocrystalline in-plane anisotropies. Therefore, the measured hysteresis loops in films grown on a MgO substrate present a rather poor squareness which gets improved as the annealing temperature increases and, consequently, as the disorder decreases. This is confirmed by a full square easy axis hysteresis loop obtained for CFA thin films annealed at 750 °C (not shown here).

B. Dynamic properties

The uniform precession and the first PSSW modes have been observed in perpendicular and in-plane applied field configurations for the 50 nm thick films, while for the 10 nm thick film, no PSSW mode is detected due to their high frequency over-passing the available bandwidth (0–24 GHz).

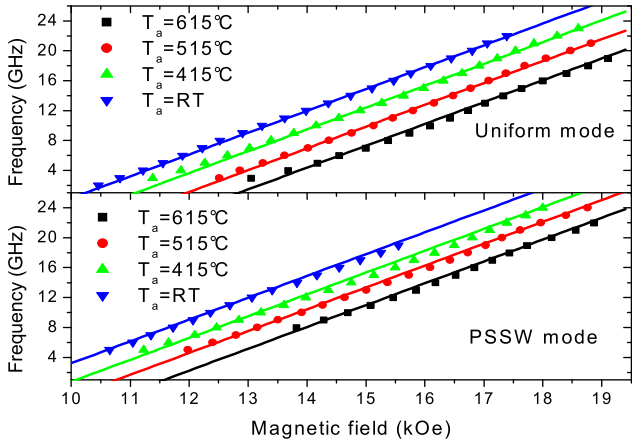

FIG. 3. Variation of the frequencies of the uniform and PSSW modes for 50 nm thick CFA films annealed at different temperatures. Solid lines indicate the fit using the model described in the text.

Typical perpendicular field dependences of the resonance frequencies of the uniform and of the PSSW modes are shown on Figure 3 for the CFA film grown on Si. By fitting the data in Figure 3 to the model presented above, the gyromagnetic factor (γ), the exchange stiffness constant (A_{ex}), and the effective magnetization ($4\pi M_{eff}$) are extracted. The fitted $\gamma/2\pi = 29.2$ GHz/T is independent on T_a, while A_{ex} (Fig. 4(b)) increases versus T_a, suggesting an enhancement of the chemical order when the annealing temperature increases, presumably due to the enhancement of the chemical order. A similar behaviour of the exchange stiffness of $Co_2FeAl_{0.5}Si_{0.5}$[13] with T_a has been reported by Trudel *et al.* The smaller A_{ex} values of CFA films grown on Si compared with those grown on MgO are another indication of the better crystalline structure and chemical order of these latter.

Interestingly, the extracted effective magnetization from the MS-FMR measurements, shown in Figure 4(a), increases linearly with the annealing temperature leading to negative perpendicular anisotropy, which tends to favour the in-plane orientation. This effect is more pronounced for the 10 nm thick film: The slope of this linear dependence, in the range 415 °C–615 °C, decreases from 32 Oe/°C to 9 Oe/°C, respectively, for the 10 nm and for the 50 nm thick CFA films grown on Si. The 50 nm CFA thick film shows a larger slope (13 Oe/°C) compared with the similar CFA film grown on Si. This effect originates from the CFA/MgO interface, which is improved by increasing the annealing temperature. Moreover, a linear variation of $4\pi M_{eff}$ as function of the thickness inverse of CFA films, annealed at $T_a = 600$ °C and deposited on MgO[6] and on Si substrates, has been observed. This thickness dependent anisotropy was also observed in structures based on CoFeB/MgO,[14] but unlike CFA/MgO, the CoFeB/MgO interface favours a perpendicular magnetization. Moreover, it is worth mentioning in the case of Ta/CFA/MgO multilayers, the surface anisotropy favours also perpendicular magnetization.[15]

Figure 5 shows the typical MS-FMR angular dependence of the resonance field at 7 GHz and 8 GHz driven frequencies for three investigated CFA thick films annealed at various T_a. For the 50 nm CFA thick film grown on MgO, the angular dependence is only presented at $T_a = 615$ °C for

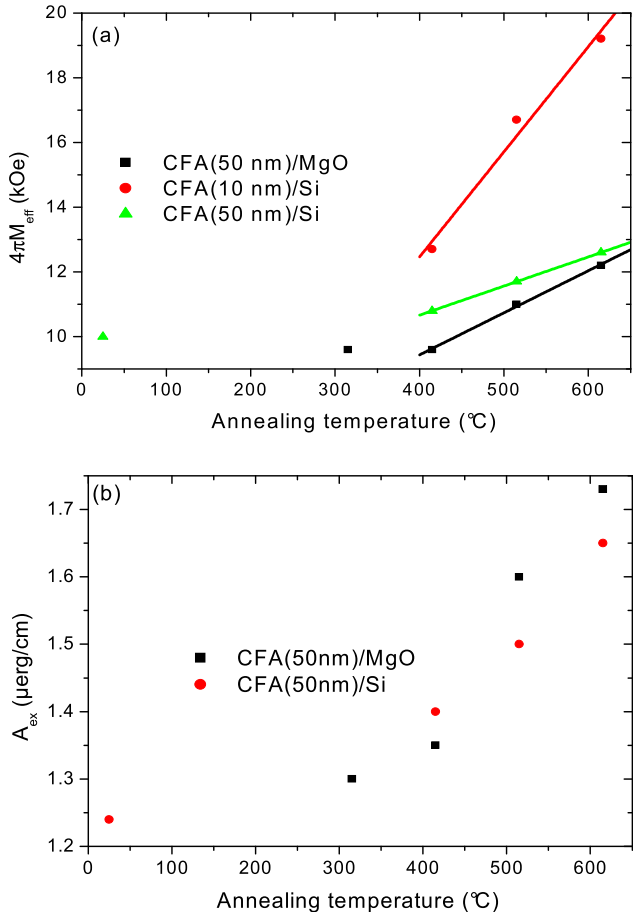

FIG. 4. Variations of (a) the effective magnetization ($4\pi M_{eff}$) and of the (b) exchange stiffness constant (A_{ex}), as function of the annealing temperature, of 10 nm and 50 nm thick CFA films grown on Si and on MgO substrates. The solid lines refer to the linear fit in the range 400–650 °C.

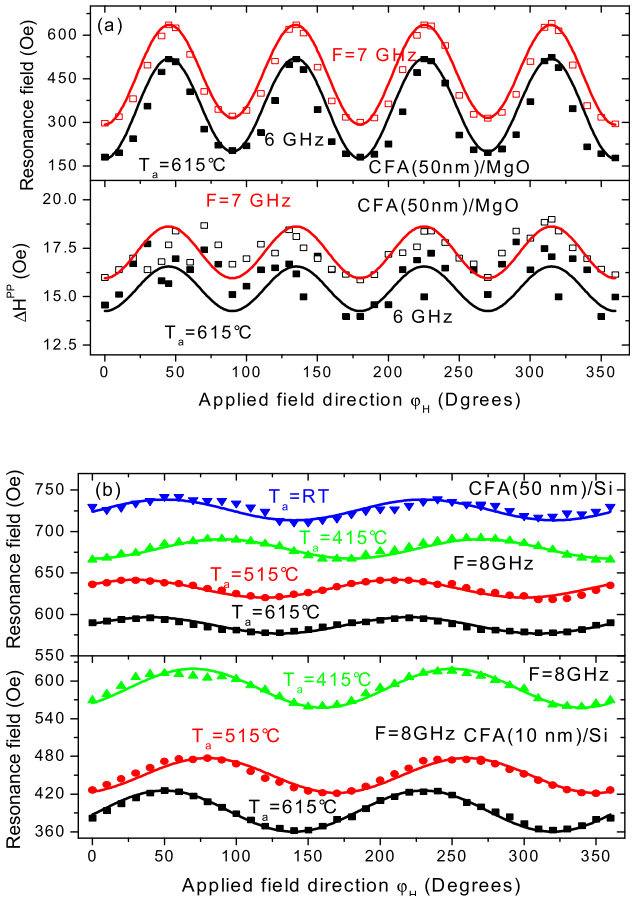

FIG. 5. Angular dependence of the resonance field and of the peak-to-peak field FMR linewidth (ΔH^{PP}) of 10 nm and 50 nm thick Co_2FeAl thin films grown on (a) MgO and on (b) Si substrates. The solid lines refer to the fit using the model described in the text.

clarity. The MS-FMR measurements show that the angular behavior of the resonance field is governed by a uniaxial anisotropy or a superposition of uniaxial and fourfold anisotropies, respectively, for films grown on Si and on MgO substrates. The disappearance of the fourfold anisotropy for CFA grown on Si is directly correlated to their in-plane polycrystalline structure due to the amorphous SiO_2 layer. The uniaxial anisotropy field (H_u), presented on Figure 6(b), is unaffected by T_a for all the samples. However, in contrast, for the CFA films grown on MgO, the direction of the uniaxial anisotropy easy axis (φ_u), varies with T_a in the case of films grown on Si substrates, as shown on Fig. 6(a), which complicates the identification of its origin. Therefore, a completely satisfactory interpretation of the presence of H_u and of its T_a dependency is still missing. For the 50 nm CFA thick film grown on MgO, the uniaxial and the fourfold anisotropies show parallel easy axes which remain independent of T_a: this common axis coincides with one of the substrate edges ($\varphi_u = \varphi_4 = 0°$) and, consequently, with one of the $\langle 110 \rangle$ crystallographic directions of the CFA phase. The decrease in the fourfold anisotropy field (H_4) as T_a increases (Fig. 6(c)) is an effect of the improving crystalline structure and of the enhancement of the chemical order.

The FMR linewidth is a measure of the relaxation rate of the magnetization and is related to the magnetic damping. This linewidth is caused by two mechanisms: the intrinsic damping of the magnetization and extrinsic contributions[16] (such as two magnon scattering, mosaicity,…). The angular and frequency dependences of the FMR linewidth provide information about these magnetic damping mechanisms.

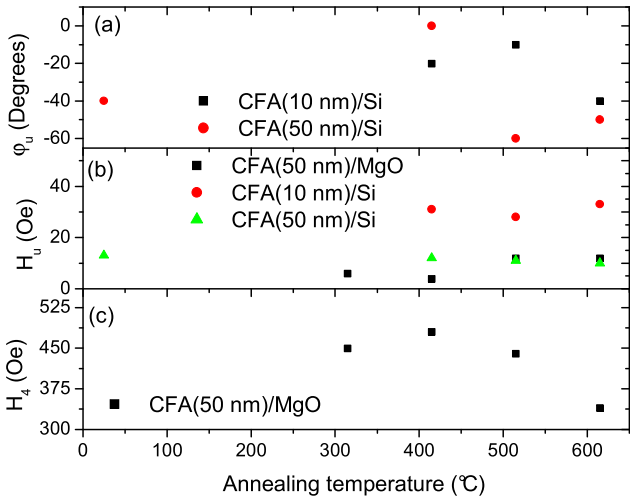

FIG. 6. Annealing temperature dependence of the (a) uniaxial anisotropy easy axis direction, (b) uniaxial (H_u), and (c) fourfold anisotropy fields (H_4) of the 10 nm and 50 nm CFA thick films grown on Si and MgO substrates.

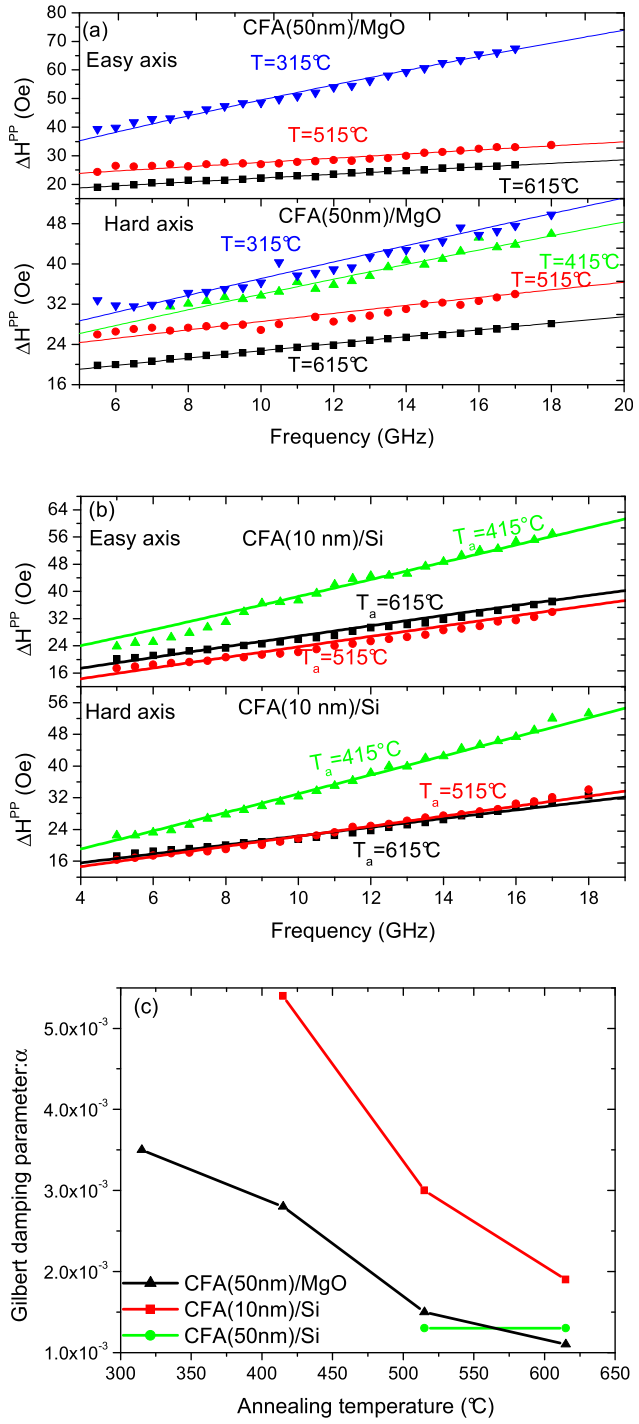

FIG. 7. Frequency dependence of the easy and of the hard axes peak-to-peak field FMR linewidth (ΔH^{PP}) for (a) 50 nm Co_2FeAl thick films grown on MgO and for (b) 10 nm Co_2FeAl thick films grown on Si. The solid lines refer to the fit using the model described in the text. (c) Annealing temperature dependence of the Gilbert damping parameter of 10 nm and 50 nm CFA thin films grown on Si and MgO substrates.

Therefore, the field peak-to-peak FMR linewidth, defined as the field difference between the extrema of the sweep-field measured FMR spectra, has been investigated as function of the annealing temperature.

In Figure 5(a), the FMR peak-to-peak linewidth (ΔH^{PP}) is plotted as a function of the field angle φ_H, using 6 GHz and 7 GHz driving frequencies, for the 50 nm CFA films grown on a MgO substrate and annealed at 615 °C. In the CFA samples grown on MgO, the ΔH^{PP} angular variation shows a perfect fourfold symmetry (in agreement with the variation of the resonance position) while it shows a uniaxial behaviour in the case of CFA grown on Si. Such behavior is characteristic of a two magnon scattering contribution. This effect is correlated to the presence of defects preferentially oriented along specific crystallographic directions, thus leading to an anisotropic damping. All the other samples show a qualitatively similar behaviour to one of the samples presented here. The positions of the extrema depend on the sample. The observed pronounced anisotropy of the linewidth cannot be due to the Gilbert damping contribution, which is expected to be isotropic, and must be due to additional extrinsic damping mechanisms.

TABLE I. Magnetic damping parameters obtained from the best fits to our experimental FMR results using the model described in the text. np: not pertinent.

d (nm)	Γ_0	Γ_1	Γ_2	φ_2 (deg)	φ_4 (deg)	ΔH^{inh}(Oe)	α	T_a (°C)
MgO substrate								
50	11	np	−1	np	0	15.2	1.1×10^{-3}	615
50	8	np	−1	np	0	20	1.5×10^{-3}	515
50	29	np	17	np	0	20	3.5×10^{-3}	315
Si substrate								
10	35	13	np	−40	np	11	1.9×10^{-3}	615
10	12	−8	np	−10	np	8.5	3×10^{-3}	515
10	31.5	−7.5	np	−20	np	1	5.4×10^{-3}	415

Figure 7 presents the frequency dependence of FMR linewidth, for an applied field parallel to the easy and the hard axes, of 50 nm and 10 nm thick CFA films annealed at various temperatures and grown, respectively, on MgO and Si substrates. It shows that the linewidth decreases with increasing T_a due to the enhancement of the chemical order. The observed angular and frequency dependences of the field linewidth have been analyzed conjointly by considering intrinsic (Gilbert), two magnon scattering, and inhomogeneities contributions, using the method described in Ref. 6 for a fit of FMR data using expression (3). Consequently, Γ_0, Γ_2, Γ_4, φ_2, and φ_4, which describe the two magnon contribution, are listed in Table I, which also contains the parameters describing the other damping effects. Figure 7(c) shows the T_a dependence of the Gilbert damping constant (α). The CFA films grown on MgO present a smaller damping parameter compared with those grown on Si. The 50 nm thick CFA film, annealed at 615 °C, shows a very low α, equal to 0.0011, which is comparable with that of the epitaxial $Fe_{0.73}V_{0.27}$, which is considered as the ferromagnetic metal having the lowest α.[17] However, the 10 nm thick sample shows relatively large values of α which decrease with increasing T_a. The reason for both these larger values for thinner films and for the decrease in α with increasing T_a, is most probably due to increase in the chemical order degree.[18]

V. CONCLUSION

Co_2FeAl films with thicknesses of 10 nm and of 50 nm were prepared by sputtering on Si(001)/SiO_2 and MgO(001) substrates and annealed at various temperatures. They show

a polycrystalline structure and an epitaxial growth when Si and MgO substrates are used, respectively. The chemical order changes from A2 structure to B2 when increasing the annealing temperature (T_a). The microstrip MS-FMR has been used to study the dynamic properties. The MS-FMR has been adjusted to a model allowing for the determination of the most relevant parameters. The in-plane uniaxial anisotropy field, present in all the samples, is unaffected by T_a and the fourfold anisotropy field, observed in the sample grown on MgO, decreases when increasing the annealing temperature. The presence of this fourfold anisotropy is directly correlated to the crystalline structure of CFA grown on MgO. The effective magnetization increases drastically with T_a, due to the enhancement of the CFA/MgO interface quality. The angular and frequency dependences of the FMR linewidth, which decreases with increasing annealing temperature, are governed by two magnon scattering and by a Gilbert damping which decreases with the increasing annealing temperature due to the chemical disorder.

ACKNOWLEDGMENTS

This work was partially supported by POS CCE Project ID.574, code SMIS-CSNR 12467, and "SPINTAIL" PN-II-ID-PCE-2012-4-0315.

[1]H. C. Kandpal, G. H. Fecher, and C. Felser, J. Phys. D **40**, 1507 (2007).
[2]R. A. de Groot, F. M. Mueller, P. G. van Engen, and K. H. J. Buschow, Phys. Rev. Lett. **50**, 2024 (1983).
[3]W. H. Wang, H. Sukegawa, and K. Inomata, Phys. Rev. B **82**, 092402 (2010).
[4]W. H. Wang, H. Sukegawa, R. Shan, S. Mitani, and K. Inomata, Appl. Phys. Lett. **95**, 182502 (2009).
[5]S. Picozzi, A. Continenza, and A. J. Freeman, Phys. Rev. B **69**, 094423 (2004).
[6]M. Belmeguenai, H. Tuzcuoglu, M. S. Gabor, T. Petrisor, Jr., C. Tiusan, D. Berling, F. Zighem, T. Chauveau, S. M. Chérif, and P. Moch, Phys. Rev. B **87**, 184431 (2013).
[7]M. S. Gabor, T. Petrisor, Jr., C. Tiusan, M. Hehn, and T. Petrisor, Phys. Rev. B **84**, 134413 (2011).
[8]K. Inomata, N. Ikeda, N. Tezuka, R. Goto, S. Sugimoto, M. Wojcik, and E. Jedryka, Sci. Technol. Adv. Mater. **9**, 014101 (2008).
[9]H. J. Elmers, S. Wurmehl, G. H. Fecher, G. Jakob, C. Felser, and G. Schönhense, Appl. Phys. A **79**, 557 (2004).
[10]M. Belmeguenai, F. Zighem, Y. Roussigné, S. M. Chérif, P. Moch, K. Westerholt, G. Woltersdorf, and G. Bayreuther Phys. Rev. B **79**, 024419 (2009).
[11]B. Heinrich and J. F. Cochran, J. Appl. Phys. **57**, 3690 (1985).
[12]A. K. Srivastava, M. J. Hurben, M. A. Wittenauer, P. Kabos, C. E. Patton, R. Ramesh, P. C. Dorsey, and D. B. Chrisey, J. Appl. Phys. **85**, 7838 (1999).
[13]S. Trudel, G. Wolf, J. Hamrle, B. Hillebrands, P. Klaer, M. Kallmayer, H. J. Elmers, H. Sukegawa, W. Wang, and K. Inomata, Phys. Rev. B **83**, 104412 (2011).
[14]S. Ikeda, K. Miura, H. Yamamoto, K. Mizunuma, H. D. Gan, M. Endo, S. Kanai, J. Hayakawa, F. Matsukura, and H. Ohno, Nature Mater. **9**, 721 (2010).
[15]M. S. Gabor, C. Tiusan and T. Petrisor, J. Appl. Phys. **114**, 063905 (2013).
[16]Kh. Zakeri, J. Lindner, I. Barsukov, R. Meckenstock, M. Farle, U. von Hörsten, H. Wende, W. Keune, J. Rocker, S. S. Kalarickal, K. Lenz, W. Kuch, and K. Baberschke, Phys. Rev. B **76**, 104416 (2007).
[17]C. Scheck, L. Cheng, I. Barsukov, Z. Frait, and W. E. Bailey, Phys. Rev. Lett. **98**, 117601 (2007).
[18]S. Mizukami, D. Watanabe, M. Oogane, Y. Ando, Y. Miura, M. Shirai, and T. Miyazaki, J. Appl. Phys. **105**, 07D306 (2009).